Article ID: 1003－6326(2004)03－0485－06

Effect of sintering on microstructures and properties of sub-micron Ti(C, N)-based cermets①

YU Li-xin(余立新)[1], XIONG Wei-hao(熊惟皓)[1, 2], ZHENG Yong(郑 勇)[3], LI Guo-an(李国安)[1]
(1. State Key Laboratory of Die & Mould Technology, College of Materials Science and Engineering, Huazhong University of Science and Technology, Wuhan 430074, China;
2. State Key Laboratory of Advanced Technology for Materials Synthesis and Processing, Wuhan Universty of Technology, Wuhan 430070, China;
3. College of Materials Science and Engineering, China Three Gorges University, Yichang 443002, China)

Abstract: The influence of different sintering processes, including vacuum sintering, vacuum sintering followed by HIP and sintering-HIP, on the microstructure and properties of sub-micron Ti(C, N) cermets with various binder contents was studied. Image analysis based on back-scattered electrons image observations was used to determine the morphologic and structural characteristics. Transverse rupture strength(TRS), hardness, fracture toughness were measured and TRS data were treated by Weibull statistics further. It is shown that a very significant improvement in TRS can be obtained by HIP or sintering-HIP treatment for the alloys with lower and middle binder content at the controlled cooling rate, but the effect is not obvious for the alloys with higher binder content. HIP is also helpful for improving the hardness of sub-micron Ti(C, N) cermets, however, but can lower the fracture toughness. The variation of these properties was interpreted in terms of the difference in morphologic and structural characteristics.

Key words: Ti(C, N) cermet; sub-micron; sintering process; HIP
CLC number: TG 148 **Document code:** A

1 INTRODUCTION

Compared with WC-Co hardmetals, Ti(C, N) based cermets have many advantages: lower density, higher oxidation resistance, higher thermal expansion coefficient, higher high-temperature hardness, reasonable strength at elevated temperature and higher wear resistance. Therefore, Ti(C, N) based cermets can be used as indexable inserts and wear resistance parts. A lot work has been done on Ti(C, N) based cermets in recent years, and the applications in some fields are quite successful. At present, at least 20% of all indexable inserts used in Japan are Ti(C, N) based cermets[1]. However, the transverse rupture strength(TRS) and fracture toughness(K_{IC}) of Ti(C, N) based cermets are comparably lower than those of WC-Co hardmetals.

Several methods have been used to improve the properties of Ti(C, N) based cermets. Appropriate chemical compositions, in which Ni was partially replaced by Co[2, 3], and carbides and carbon-nitrides of W, Ta, Nb or V were added, can ameliorate the properties of Ti(C, N) based cermets[4-7]. The carbon and nitrogen contents are also important for achieving higher performance[8]. Sub-micron Ti(C, N) based cermets possess superior transverse rupture strength, hardness, fracture toughness[9-12].

Hot isostatic pressing (HIP) was applied in the production of cemented carbides in 1960s. It was reported that the properties of cemented carbides could be improved a lot because of the elimination of the flaws in the parts[13]. In 1980s, a simultaneous sintering and HIP treating equipment, called sintering-HIP(SH) was developed in the production of cemented carbides. The advantage for SH is that the binder "lakes" typically resulted from HIP can be avoided, and at the meanwhile energy can be saved to some extent[14]. The manufacturing procedure of Ti(C, N) based cermets is similar to that of cemented carbides. It is assumed that the HIP and SH treatment on Ti(C, N) based cermets have similar effects on cemented carbides. A few papers[2, 15] on HIP treated Ti(C,

① **Foundation item:** Project(50074017) supported by the National Natural Science Foundation of China; Project (992P0332) supported by the Key Science and Technology Development Foundation of Hubei Province, China; Project supported by the State Key Laboratory of Advanced Technology for Materials Synthesis and Processing, China
Received date: 2003－09－08; **Accepted date:** 2003－11－25
Correspondence: YU Li-xin, PhD; Tel: +86-728-6518287; E-mail: yulixin@kingdream.com

N) based cermets have been published, but only the final mechanical properties were reported, without highlighting the process and microstructural characteristics of different grades of Ti(C, N) based cermets. Furthermore, few work has been reported on SH treated Ti(C, N) based cermets. The aim of this paper is to investigate the effect of sintering process, including VS(vacuum sintering), VS+ HIP and SH, on the microstructure and properties of sub-micron Ti(C, N) based cermets with different binder contents.

2 EXPERIMENTAL

The compositions of the cermets in the present study are given in Table 1. Test specimens were prepared by the conventional powder metallurgy procedure, i.e. attritor ball milling followed by compaction and sintering. The details was reported elsewhere, and these Ti(C, N) based cermets was characterized by sub-micron structure[16].

Table 1 Nominal compositions of alloys (volume fraction, %)

Alloy	TiC	TiN	WC	Mo	Ni
A	68.4	11.4	2.6	10.6	7.0
B	59.3	12.2	2.7	11.0	14.8
C	45.8	13.1	2.9	10.4	27.8

Materials were sintered by three kinds of sintering procedures, VS, VS+ HIP and SH. VS was carried out in vacuum furnace at 1 450 ℃ for alloy A, 1 420 ℃ for alloy B and 1 390 ℃ for alloy C for 1.5 h at the pressure of 10 Pa. These VS test specimens were then subjected to HIP in QIH-6 HIP furnace at 1 320 ℃ and a pressure of 103 MPa, with a cooling rate of 10 ℃/min. In order to investigate the effect of HIP temperatures on the microstructures and properties of the samples, the HIP treatment of alloy B was also carried out at 1 290 ℃ and 1 350 ℃, respectively. In order to investigate the effect of the cooling rate on the microstructure and properties, the consequently cooling rate of alloy B after HIP at 1 320 ℃is also controlled at 25 ℃/min. The SH treatment of alloys A, B and C was carried out in UT-500 sintering furnace at 1 420 ℃, and the sintering pressure is controlled at 1.8 MPa.

The TRS(σ_r) values were measured according to the Standard ISO3327. In order to provide a better statistical indication of the TRS distribution, TRS data were treated by the Weibull method[13]. For each group of specimens, TRS values were arranged in increasing order and the factor P was calculated from the rank order using the equation as

$$P = j/(N+1) \quad (1)$$

where P represents probability factor, j rank order (for $\sigma_{r,\min}$, $j=1$), and N total number of values in group.

Data were then plotted as $\ln(\ln(1/(1-P)))$ vs $\ln(\sigma_r/\mathrm{MPa})$. The slope of the plot, m, is called Weibull modulus. Such plot has the following characteristics: sets of data with higher consistency have higher m value, and the materials with higher strength have Weibull curves lying farther to the right on the plot.

The polished specimens were used to evaluate the porosity, Vickers hardness, indentation fracture toughness, and microstructural parameters. The porosity of alloy was determined by optical microscope (OM) according to ASTM B276-91.

Hardness of the sintered compacts was measured by a HVS-50 Vickers hardness testing machine according to ISO3878. Vickers hardness was calculated by the equation as

$$HV_{30} = 55.63/d^2 \quad (2)$$

where d is the mean diagonal of indentation, mm.

Indentation fracture toughness was measured according to the method suggested by Shetty et al[17]:

$$K_{IC} = 0.15\sqrt{\frac{HV_{30}}{\sum l}} \quad (3)$$

where $\sum l$ is the sum of crack lengths, mm.

The polished specimens were observed by a JSM-5600LV scanning electron microscope in back-scattered electron imaging mode. For each specimen, about 10 back-scattered electron images (BEI) were taken arbitrarily from various locations and were used subsequently for quantitative metallographic study.

The software of quantitative metallographic analysis was developed by Nanjing Transcend New-Tech Co. Ltd, China. The various microstructural parameters, namely, carbide mean linear intercept grain size, contiguity, and binder mean linear intercept distance, were calculated using the following equations.

The carbide mean liner intercept grain size can be expressed as

$$L_\gamma = \frac{2\varphi_\gamma}{2(N_{\gamma/\gamma}) + N_{\gamma/\beta}} \quad (4)$$

where φ_γ is the volume fraction of the carbide phase, $N_{\gamma/\beta}$ and $N_{\gamma/\gamma}$ are the average numbers of intercepts per unit length of test lines with traces of the carbide/binder interface and carbide/carbide grain boundaries respectively.

The contiguity of the carbide phase can be expressed as

$$C_\gamma = \frac{2N_{\gamma/\gamma}}{2N_{\gamma/\gamma} + N_{\gamma/\beta}} \quad (5)$$

and the binder mean linear intercept distance, i. e. the mean free path, can be expressed as

$$L_\beta = \frac{2\varphi_\beta}{N_{\gamma/\beta}} \quad (6)$$

where φ_β is the volume fraction of the binder phase.

3 RESULTS AND DISCUSSION

3.1 Effect of sintering procedures on microstructures

The back-scattered electron images of alloy A sintered with different procedures are presented in Fig. 1. Similar microstructures can be observed from Fig. 1. The dark phases called γ' phase with the composition of $Ti(C_{1-x}, N_x)$ are the cores of the carbonitride grains. The grey phases called γ'' with the composition of $(Ti_{1-y-z}, Mo_y, W_z)(C_{1-x}, N_x)$ are the rim phase nucleated and grown during sintering in coherence with the γ' core. The rim phases have two kinds of forms. One is brighter inner rim enriched with higher W or Mo content, which surrounds the core and is formed during solid state sintering. The other is grey outer rim precipitated from the binder phase after the eutectic temperature is reached[6]. The symbol γ is used to designate the phases γ' and γ'', when no distinction between the two phase is needed. The metallic binder phase is called β phase. It generally appears brighter than the rim.

However, the quantitative metallographic study shows there are some differences in the structural parameters. The main results determined by the image analysis are given in Table 2.

Compared with VS alloy, the γ' core of HIP alloy is smaller in size, and the volume fraction of γ' core is slightly decreased; as a whole of rim and core, the size of hard phase γ is slightly larger. The variation of volume fraction of β binder phase is not conspicuous, but the binder mean linear intercept distance increases apparently, resulting in the increase of the contiguity. The microstructural parameter variations of HIP alloys are due to the reaction of diffusion, dissolution and reprecipitation during reheating. When alloy is subjected to HIP treatment, a part of

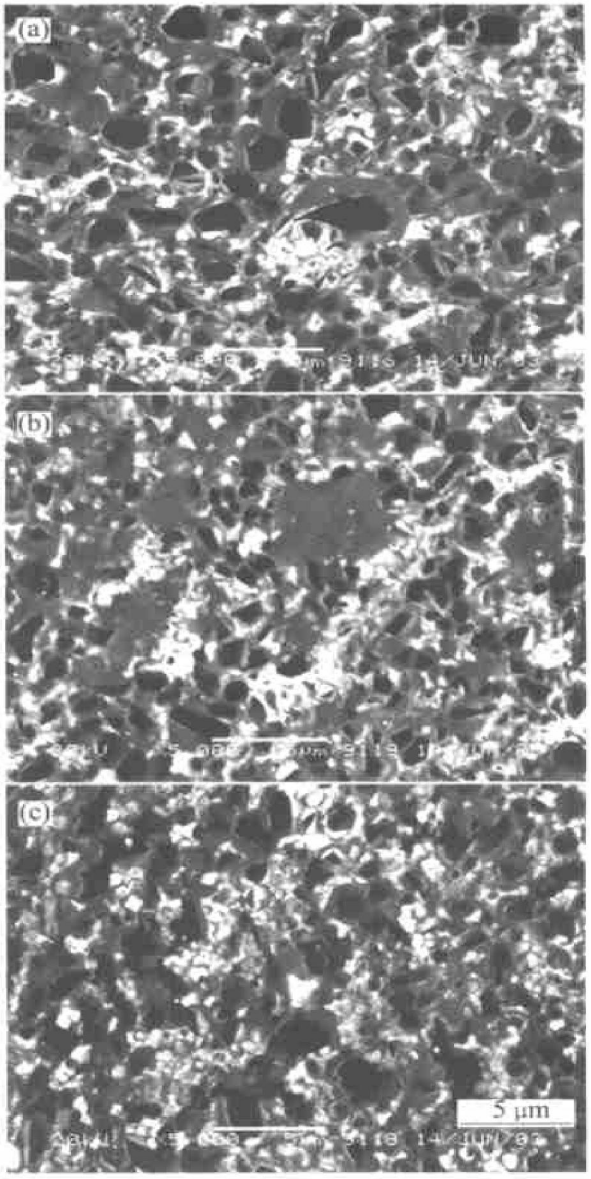

Fig. 1 Back-scattered electron images of alloy A after different sintering procedures
(a) —VS; (b) —VS+ HIP; (c) —SH

γ' core are dissolved in the binder transported by diffusion and reprecipitated to the larger hard grains with a composition given by the equilibrium conditions(outer rim). After the liquid forms, further dissolution and reprecipitation occur. The dissolution of the smaller γ phase grain continues forming the γ'' rim around the bigger grain[18].

Table 2 Microstructural parameters of alloy A after different sintering procedures

Sintering process	Volume fraction calculated from image analysis/%			Mean diameter/μm		$N_{\gamma/\beta}$/μm	Contiguity of γ grain
	Core γ'	Rim γ''	Binder β	Core	Rim+ Core	Binder β	
VS	19.40	70.22	10.38	0.52	0.71	0.22	57.04
VS+ HIP	17.89	71.98	10.13	0.45	0.78	0.25	62.71
SH	18.39	69.80	11.81	0.48	0.70	0.20	53.04

The volume fraction of β binder phase of the cermets sintered by VS is lower than that of the cermets sintered by SH, accompanied by an increase in the contiguity. This is resulted from the higher vapor pressure of nickel at the sintering temperature, and consequently considerable loss of the nickel binder under vacumm sintering condition. The loss of nickel in practice has been reported up to 10% or more[19]. But the UI－500 sintering-H2P furnace has binder loss protect system, and the vapor of nickel has been depressed in SH procedure.

No matter what kind of sintering procedures are applied, the γ″ rim are the predominant phase, occupying a volume fraction nearly up to four times bigger than that of the γ′ cores.

Alloys B and C have similar microstructures as alloy A, but there are higher β binder phase volume fraction and lower γ′ cores volume fraction than alloy A. Quantitative metallographic study reveals that, after VS procedure, the volume fraction of β binder phase is about 17% and that of γ′ cores is also about 17% in alloy B. The volume fraction of β binder phase is about 28% and that of γ′ cores is 14% in alloy C. The effect of sintering procedures on the microstructural parameters is similar to that of alloy A.

3.2 Effect of sintering process on TRS

Weibull plots of TRS for alloys A, B and C produced by different sintering procedures are shown in Figs. 2－4.

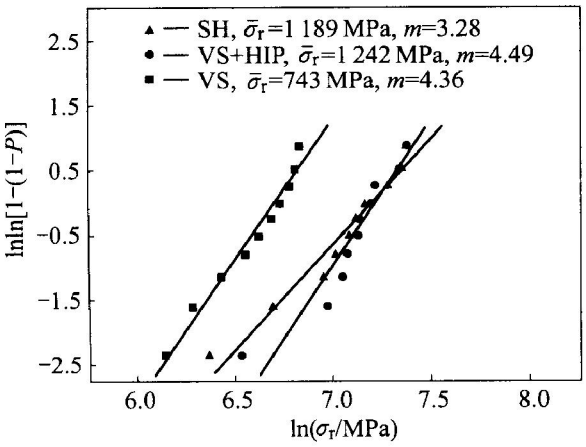

Fig. 2 Weibull plot of TRS of alloy A treated by different sintering procedures

Figs. 2 and 3 provide excellent confirmation of the benefit of SH and HIP for lower and middle binder content alloys. Compared with Weibull curves of VS specimen, specimens subjected to SH and HIP show a strong improvement (about 60%－90%) in TRS. Both the average TRS values and the reliability (Weibull modulus) are increased if the cooling rate is under control. This is mainly due to the elimination

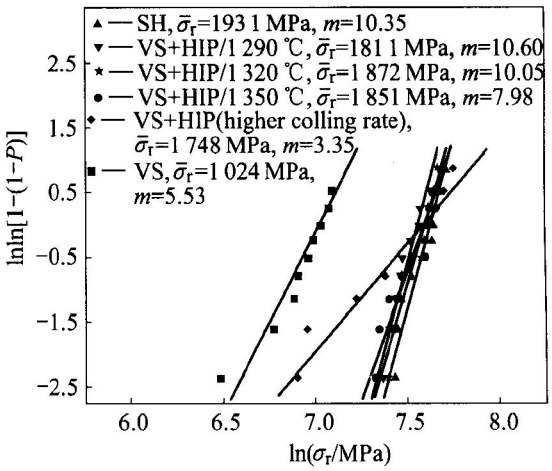

Fig. 3 Weibull plot of TRS of alloy B treated by different sintering procedures

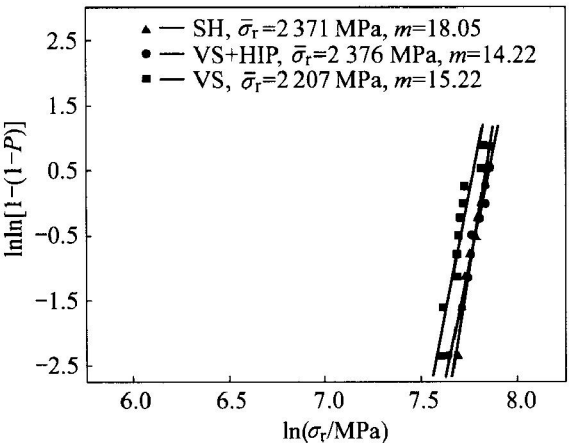

Fig. 4 Weibull plot of TRS of alloy C treated by different sintering procedures

of porosity in specimens subjected to SH and HIP sintering procedure. The porosity distributions of alloys A and B under vacuum sintering are similar, i. e. A_{06} B_{06}, but the porosity distribution of alloys subjected to SH and HIP decreased to $A_{02}B_{02}$.

Fig. 2 also shows that the VS+ HIP procedure is more effective to improve the TRS of alloy A than SH procedure, but Fig. 3 shows the opposite result for the alloy B. It seems that the sintering pressure at SH procedure, 1. 8 MPa, is not enough to minimize the porosity of the lower binder content alloy A to some extent. But it is enough for the middle binder content alloy B, and the binder "lakes" can also be avoided[20].

Compared with alloys A and B, the effect of HIP and SH on alloy C is much less pronounced. This is due to its higher fracture toughness of alloy C. In addition, alloys with higher nickel content can be manufactured more easily with lower defect levels.

TRS data for alloys A, B and C show that the maximum TRS and the Weibull modulus of each grade increase with increasing nickel content.

Fig. 3 also shows that there is no definite distinction among the effects of the HIP temperatures on TRS within the statistical limitation. Substantial improvement in TRS is obtained under different HIP temperatures. However, the value of Weibull modulus(m) is much lower when the cooling rate is higher, e. g. at 25 ℃/min. It is shown that the cooling rate is critical to obtain higher mechanical properties. There may be two ways by which the cooling rate affects the mechanical properties of alloys. One is that higher cooling rate results in higher stress in the specimens due to the difference of thermal conductivity and thermal expansion coefficient between hard phase and nickel binder. The other is that the cooling rate affects the structure of grain boundaries. When the cooling rate is too higher, the micro-crystal layer in the interface of the rim and the metallic phase is not completed, and the TRS is relatively lower[21].

3.3 Effect of sintering process on Vickers hardness and indentation fracture toughness

The Vickers hardness and indentation fracture toughness are observed to be related to the variation of the microstructure and compositions.

The values of the hardness of alloys A, B and C under different sintering procedures are shown in Fig. 5. Higher hardness of the HIP alloy can be observed compared with that of the VS alloy, and this is due to the increasing of γ phase contiguity. The VS alloy has higher hardness than SH alloy because of the remarked evaporation of nickel during the vacuum sintering.

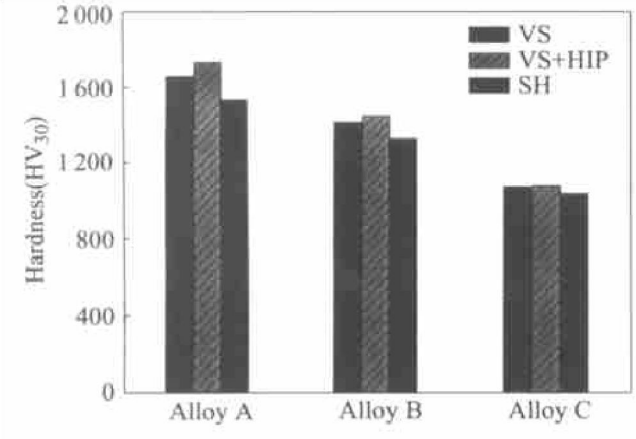

Fig. 5 Vickers hardness values of alloys A, B and C treated by different sintering procedures

The indentation fracture toughness values of alloys A and B under different sintering conditions are shown in Fig. 6. Because the alloy C has higher content of binder phase and the crack lengths is too short to determine the indentation fracture toughness,

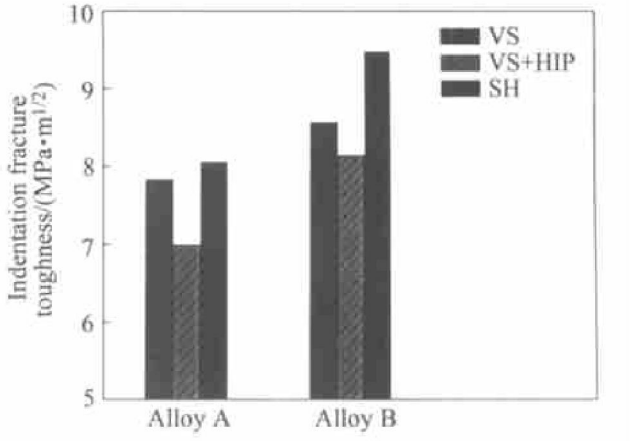

Fig. 6 Indentation fracture toughness values of alloys A and B treated by different sintering procedures

there is not indentation fracture toughness value for alloy C. The indentation fracture toughness of the alloy by SH is slightly higher than that of the VS alloy because of its higher nickel binder content. HIP alloy has lower indentation fracture toughness because of its larger γ phase size and contiguity[12].

4 CONCLUSIONS

1) Relationship between the microstructural parameters and the properties of sub-micron Ti(C, N) based cermets prepared by different sintering procedures show that HIP alloys can be characterized by smaller size of γ′ core, but larger size of γ phase, higher mean linear intercept distance of binder accompanied by higher contiguity and thus the higher hardness values.

2) The transverse rupture strength values of the sub-micron Ti(C, N) cermets with lower and middle binder content can be improved remarkably with HIP and SH treatment, because of the resulted lower porosity level.

3) It is shown that the properties of the alloys with higher nickel content are not sensitive to the treatment of HIP and SH. This can be attributed to a substantially larger transverse rupture strength value and lower as-sintered defect level of the alloys.

4) The effect of HIP temperatures on the microstructure and properties of sub-micron Ti(C, N) based cermets is not conspicuous, but the cooling rate is proved vitally important in improving the transverse rupture strength of sub-micron Ti(C, N) based cermets.

REFERENCES

[1] Clark E B. Extending the application areas for titanium carbonitride cermetss [J]. International Journal of RM&HM, 1992, 11: 23-33.

[2] Ettmager P. Ti(C, N) cermets metallurgy and properties

[J]. International Journal of RM&HM, 1995, 13: 343 - 351.

[3] Lindal P. Atom-probe analysis of the binder phase in TiC-TiN-Mo_2C-(Co/Ni) cermets[J]. International Journal of RM & HM, 1993 - 1994, 12: 115 - 119.

[4] Rolander U, Weinl G, Zwinkels M. Effect of Ta on structure and mechanical properties of (Ti, Ta, W)(C, N)-Co cermets[J]. International Journal of RM & HM, 2001, 19: 325 - 328.

[5] Lindal P, Rosen A E, Gustafson P, et al. Effect of pre-alloyed raw materials on the microstructure of (Ti, W)(C, N)-Co Cermet[J]. International Journal of RM & HM, 2000, 18: 273 - 279.

[6] Lindal P, Gustafson P, Rolander U, et al. Microstructure of model cermets with high Mo or W content[J]. International Journal of RM & HM, 1999, 17: 411 - 421.

[7] Viatte T, Bolognini S, Cutard T, et al. Investigation into the potential of a composite combining toughness and plastic deformation resistance[J]. International Journal of RM & HM, 1999, 17: 79 - 89.

[8] Zackrisson J, Andren H O. Effecet of carbon content on the microstructure and mechanical properties of (Ti, W, Ta, Mo)(C, N)-(Co-Ni) cermets[J]. International Journal of RM & HM, 1999, 17: 265 - 273.

[9] Eqami E A. Mechanical properties and microstructures of submicron cermets [J]. International Journal of RM&HM, 1995, 13: 313 - 314.

[10] Jeon E T, Joardar J, Kang S. Microstructure and tribo-mechanical properties of ultrafine Ti(C, N) cermets[J]. International Journal of RM & HM, 2002, 20: 207 - 211.

[11] Laoui T. Analytical electron microscopy of the core/rim structure in titanium carbonitride cermets[J]. International Journal of RM & HM, 1992, 11: 207 - 212.

[12] LI Chen-hui, YU Li-xin, XIONG Wei-hao. Effect of hard phases grain size on cermets fracture toughness[J]. Acta Materiae Compositae Sinica, 2003, 20(1): 1 - 6. (in Chinese)

[13] Larson F G, Hong J, Goodson R, et al. Hot isostatic pressing of cemented carbides[J]. International Journal of RM & HM, 1984, 3: 30 - 34.

[14] Lueth R C. Mouldless Hot pressing of cemented carbides[J]. International Journal of RM & HM, 1985, 4: 87 - 91.

[15] HE Cong-xun, XIA Zhi-hua, WANG You-ming, et al. Study of Ti(C, N)-based metal ceramic[J]. Rare Metals, 1999, 23(1): 4 - 12. (in Chinese)

[16] YU Li-xin, XIONG Wei-hao, LI Chen-hui, et al. Study of sub-micron Ti(C, N)-based cermets manufactured by attritor milling[J]. Journal of Materials Engineering, 2002, 7: 12 - 15. (in Chinese)

[17] Shetty D, Wright I, Mincer P, et al. Indentation fracture of WC-Co cermets[J]. J Mater Sci, 1985, 20: 1873 - 1882.

[18] Andren H O. Microstructure development during sintering and heat-treatment of cemented carbides and cermets [J]. Materials Chemistry and Physics, 2001, 67: 209 - 213.

[19] XIONG Wei-hao. Study on Microstructure and Interfaces of Particle Reinforced Hard Composite Materials [D]. Wuhan: Huazhong University of Science and Technology, 1994. (in Chinese)

[20] YU Li-xin, LI Chen-hui, XIONG Wei-hao. Study of Ti(C, N)-based cermets manufactured by sintering-HIP [J]. Cemented Carbide, 2001, 2: 69 - 73. (in Chinese)

[21] XIONG Wei-hao, HU Zhen-hua, CUI Kun. Formation mechanism of micro-crystal interface layer in Ti(C, N)-based cermets[J]. Acta Metallurgica Sinica, 1997, 33 (5): 473 - 478. (in Chinese)

(Edited by YANG Bing)